CHARACTERISTIC RESEARCH ON THE LIQUID PRODUCT FROM CO-HYDROTHERMAL LIQUEFACTION OF OILY SCUM AND LIGNOCELLULOSIC BIOCHAR

Shuanghui DENG, Zhicheng FU, Houzhang TAN*, Zhong XIA, Shiyin YU, Xuebin WANG

MOE Key Laboratory of Thermo-Fluid Science and Engineering, Xi'an Jiaotong University, Xi'an, Shaanxi, 710049, China

*Corresponding author: Houzhang Tan, Email: hzt@xjtu.edu.cn)

Hydrothermal liquefaction (HTL) is an effective way to treat solid wastes with high moisture content. The co-hydrothermal liquefaction (co-HTL) experiments of oily scum (OS) and poplar sawdust biochar (BC) at the different hydrothermal temperatures were performed in this work. The changes of the appearance and components of the liquid products were comprehensively studied. The results showed that the addition of BC into OS significantly reduced the moisture content of the residue hydrochars obtained after co-HTL. As the hydrothermal temperature increased, the liquid products obtained from co-HTL turned clearer and lighter in color, and the recovery rate of the liquid products significantly increased. The co-HTL of BC and OS could effectively improve the liquid quality and enhance the recovery rate of hydrochars. The carbon numbers of the liquid products obtained from co-HTL were concentrated in C5-C11, which were main compositions of gasoline. This work can provide basic data and theoretical reference for OS efficient treatment and engineering practice.

Keywords: Oily scum, Biochar, Liquefaction, Liquid, Characteristic analysis

1. Introduction

Oily sludge is produced in oilfield exploitation, transportation, storage and refining, etc. Generally, the petroleum refining process generates large amounts of refinery wastewater, while bottom sludge from the oil separation tank, oily scum (OS), and residual activated sludge, which are commonly known as three sludge products, are produced in the refinery [1, 2]. The largest proportion of three sludge products is OS, accounting for 80% [3]. The main compositions of OS generally contain water content (90-99%), waste oil (0.5-3%), and solid particles (0.2-2%) [4]. More specifically, OS includes aged crude oil, asphaltenes, heavy metals and other chemical agents [5]. As a hazardous waste, OS contains a stable water-oil structure as well as emulsification and flocculation systems, making it difficult to achieve the removal of water and consuming huge costs [6]. At present, the pre-treatment methods of plate and frame pressure filtration or centrifugal dehydration are applied for OS to obtain

filter cakes, which are sent to an incinerator to use combustible substances such as oil and other hydrocarbons. However, incineration of oily sludge including OS results in serious secondary pollutions such as the vaporization of heavy metal as well as pollution of NO_x, SO_x and particulates [7-10].

At present, hydrothermal liquefaction (HTL) is regarded as an effective thermal pre-treatment, which has a significant effect on improving OS dewatering performance [11, 12]. HTL generally takes place in a closed kettle container at a certain temperature (150-290 ℃) and self-generated pressure (2-10 MPa) [13, 14]. It can dissolve the internal flocs, destroy colloid structure, and release the intracellular water, thereby improving the dewatering performance of materials with high moisture content [15]. Duan et al. found that adding NaOH could increase the oil recovery rate to 78.6% and promote oil-water separation in the hydrothermal experiments of OS [16]. Namioka et al. found that the moisture content of sludge which was treated at 200 ℃ decreased with the increase of hydrothermal dehydration pressure [17]. Zhang et al. used sodium hypochlorite (NaClO) as well as a combination of NaClO and ultrasound for the first time to pretreat wet sludge and found that both pre-treatment methods improved the recovery rate of bio-oil, and the energy recovery rate of the liquid bio-oil obtained was as high as 58.0% [18]. However, now the high compressibility of the internal flocculent structure of OS is not completely solved when it is HTL alone, and excessive hydrothermal temperature can cause high energy consumption, darken the color of the liquid, and make it difficult to be applied. At the same time, the hydrochar properties are unstable as fuel. Now, some researchers have use biomass as an additive to improve hydrothermal product performance of sewage sludge. Cavali et al. studied the co-hydrothermal reaction of pine sawdust with wet sludge and found that the addition of pine sawdust was beneficial for improving the calorific value of hydrothermal char [19]. Shan et al. found that co-hydrothermal of rice husks with domestic sludge was beneficial for reducing the content of amine substances in hydrochars [20]. Wang et al. found that there was a synergistic effect of nitrogen enrichment between the two samples in the hydrothermal co‐carbonization of lignocellulosic biomass and sludge, which increased the nitrogen content in the hydrochars [14]. These results have indicated that different types of biomass could improve the characteristics of co-hydrothermal products derived from HTL. However, at present the research on the addition of biochar into OS in the HTL process was studied rarely. Mixing OS with biochar in the HTL process may be an effective way to solve the problem of high moisture content. The reports have showed that biochar could serve as a skeleton support and break down the flocculent groups inside sludge, while the biochar itself would participate in the reaction and improve product quality [21, 22]. It is crucial to explore the interactions between biochar and OS in co-HTL, especially in terms of the dewatering performance of OS and the changes of liquid bio-oil components.

Therefore, this work researched on the co-HTL characteristics and product properties of poplar sawdust biochar (BC) and OS in a magnetic hydrothermal reactor. The co-HTL products of BC and OS at the different temperatures were systematically studied, with a focus on the following aspects: (1) the dehydration performance of OS after co-HTL; (2) distribution characteristics of the products; (3) characteristic analysis of the liquid product. The research results can offer experimental data and useful reference for the co-HTL

performance of OS and BC as well as the clean and efficient utilization of subsequent reaction products.

2. Materials and methods

2.1. Materials preparation

Raw OS was got from a petrochemical enterprise in China. Poplar sawdust was selected from a wood treatment plant in China. According to the experimental analysis, the cellulose, hemicellulose, lignin of poplar sawdust in this work are 41.77, 25.35 and 17.24 %, respectively. Poplar sawdust was placed in a tube furnace and then heated to the constant pyrolysis temperature of 600 ℃ for 4 hours under a nitrogen atmosphere. After it was cooled to ambient temperature, the biochar (BC) product was obtained. After pyrolysis, BC samples were dried at 105 ℃ for 24 h, and then separately grinded into powder (0.2 mm) before the hydrothermal experiment.

2.2. Co-HTL experiment

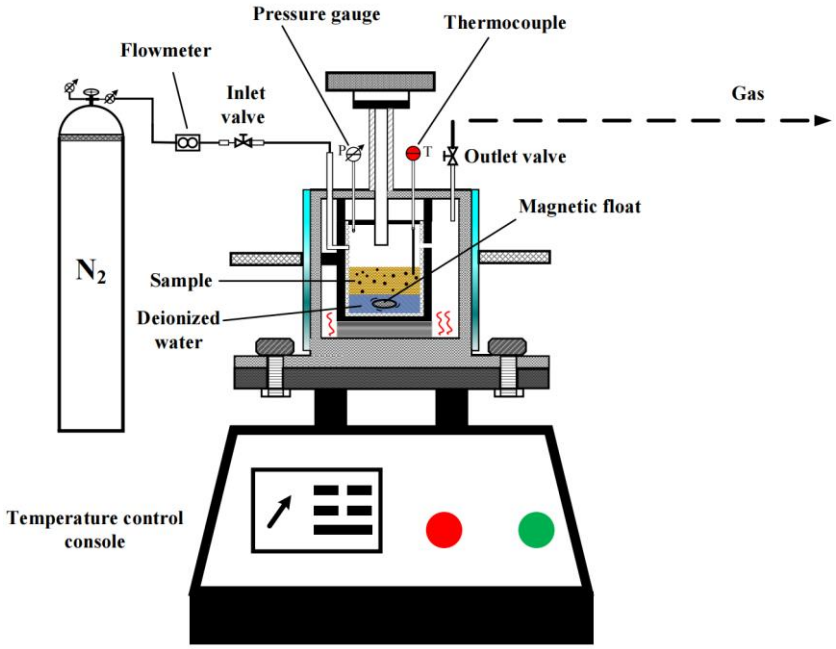

Figure 1. The HTL experimental system

The HTL experimental system is presented in Figure 1. The HTL experiments were performed in a 316 stainless steel cylinder reactor of 100 ml capacity, with an electric heater and a magnetic drive stirrer. For each mono HTL experiment of OS, 50 g of OS were placed into the reactor to mix thoroughly, and the reactor device was sealed. Before the reactor was heated, the air in the reactor was removed by nitrogen. After guaranteeing the gas tightness of the whole experimental device, the sample reactor was heated to the setting temperature (180, 200, 220, 240, 260 or 280°C) at 10 °C/min. Then, the speed of the magnetic float in the reactor was set to 300 revolutions per minute (rpm). The reaction time under each temperature kept one hour. After each experiment ended, the reactor was then cooled down to ambient temperature with cooling water. The obtained slurry product after hydrothermal experiment

was filtered via a 0.5 μm fiber membrane, and the filtrate (liquid) and wet solid products (hydrochars) were obtained. For each experiment, the obtained liquid product was placed in the glass bottle. Afterward, the wet hydrochars were dried in a heating box at 105 °C for 48 h, and the mass value of the dried hydrochars was recorded. The dried hydrochars were ground to particles and were sealed in the plastic-made bag before physicochemical property analysis. For each co-HTL experiment of OS and BC, 50 g of OS, 1 g of BC and 10 ml of deionized water were mixed together into the hydrothermal reactor. The co-HTL reaction parameters including 200, 220, 240, 260 and 280°C for 1 h at 300 rpm were applied. The co-HTL experimental procedure was same with mono HTL of OS. Each experiment was repeated at least twice to ensure reproducibility.

2.3. Analysis of liquid

A polarization microscope (BX51) was used to capture the morphology of the different liquid products. Take an appropriate amount of liquid phase sample and place it on a glass slide, cover it with a cover glass slide, and flatten the sample to make it evenly distributed, then observe it under a polarizing microscope.

A gas chromatography-mass spectrometry (GC-MS, Shimadzu GCMS-QP 2010 Ultra) was used to identify the components in the liquid from the different experimental conditions. The method of data analysis was used according to the previous testing and analyzing method [23].

2.4. Data calculation

The mass fractions of the different products were obtained by the following equations [2, 23].

$$Y_{\text{Hydrochar}}=\frac{m_{\text{Hydrochar}}}{m_{\text{Total}}}\times 100\% \quad (1)$$

$$Y_{\text{Liquid}}=\frac{m_{\text{Liquid}}}{m_{\text{Total}}}\times 100\% \quad (2)$$

$$Y_{\text{Residual moisture}}=\frac{m_{\text{Residual moisture}}}{m_{\text{Total}}}\times 100\% \quad (3)$$

$$m_{\text{Total}}=m_{\text{OS}}+m_{\text{BC}}+m_{\text{Deionized water}} \quad (4)$$

$$Y_{\text{Gas and other losses}}=1-Y_{\text{Hydrochar}}-Y_{\text{Liquid}}-Y_{\text{Residual moisture}} \quad (5)$$

Where m_{Total} is the total mass of materials which were added to the reactor, including OS, BC, and deionized water, g; $m_{Hydrochar}$ is the mass of hydrothermal carbon dried to constant weight in an oven, g; $Y_{Hydrochar}$ is the mass fraction of dried hydrochars, %; m_{Liquid} is the final mass of the collected liquid, g; Y_{Liquid} is the mass fraction of hydrothermal liquid, %; $m_{Residual\ moisture}$ is the residual moisture in hydrochars, g; $Y_{Residual\ moisture}$ is the mass fraction of residual moisture, %; and $Y_{Gas\ and\ other\ losses}$ is the mass fraction of gas and system loss during the experimental process.

The filtration characteristics are mainly reflected by the liquid percentage in the filtration process. The calculation formula of the liquid percentage is as the equation 6.

$$K_{\mathrm{r}}=\frac{m_t}{m_0}\times 100\% \tag{6}$$

$$\Delta K=K_{Co-HTL}-K_{HTL} \tag{7}$$

Where m_0 is the mass of the slurry product from the hydrothermal reaction kettle after HTL, g; m_t is the liquid mass at t time during the filtration process, g; and K_r is the liquid yield at this time. ΔK is the difference between the maximum liquid yield obtained from co-HTL of OS with BC and that obtained from OS HTL at the same hydrothermal temperature. K_{Co-HTL} is the maximum liquid yield from the co-HTL of OS with BC, K_{HTL} is the maximum liquid yield from the HTL of OS.

3. Results and discussion

3.1. Appearance changes of liquid

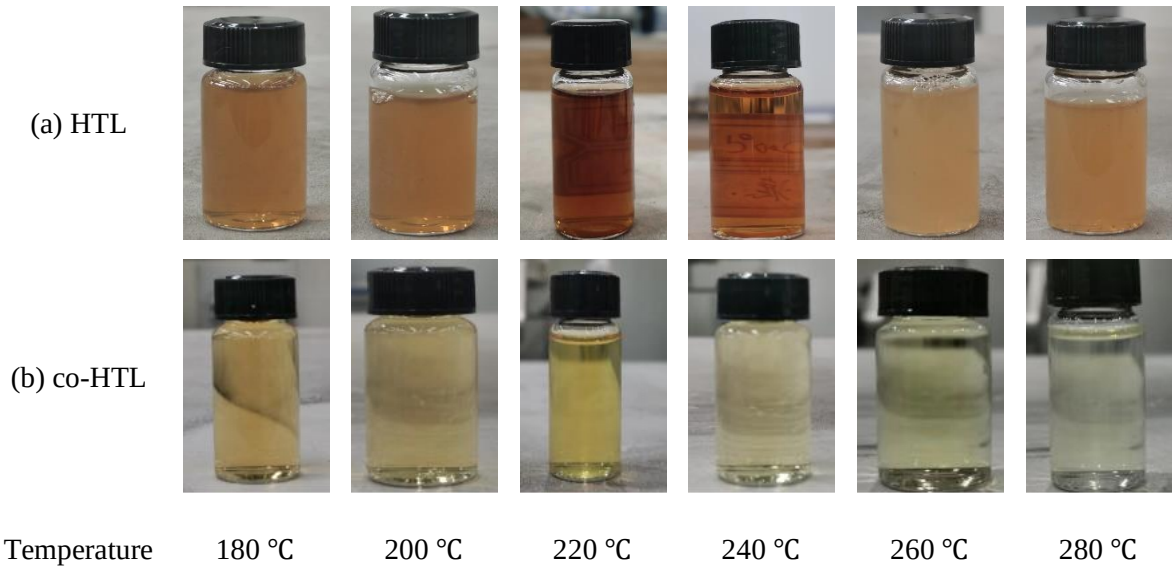

Figure 2. Color changes of the liquid products in the different conditions

The color changes of the liquid products obtained in the various experimental conditions are presented in Figure 2. In Figure 2 (a), as the hydrothermal temperature increased, the color of the liquid from OS mono HTL firstly deepened and then turned light, showing brownish black at 220 ℃. The reason may be that the organic compounds in the liquid underwent browning reactions after being heated, including Maillard reaction and caramelization reaction [24-27]. Due to the fact that the caramelization reaction was limited to the presence of only polysaccharides, the main reaction occurring during the hydrothermal process was the Maillard reaction. By observing the color changes of the liquid, the Maillard reaction mainly occurred in the temperature range of 220 to 240 ℃ when OS was hydrothermally treated alone. When the temperature reached above 260 ℃, the color of the liquid began to lighten. This was because the emulsified structure inside OS ruptured at high temperatures, causing the internal compounds to decompose. From Figure 2 (b), as the

hydrothermal temperature increased, the color of the liquid obtained from co-HTL of OS and BC turned clearer. When the hydrothermal temperature was more 240 ℃, the color of the liquid almost completely disappeared, like water from the exterior look of the liquid. This was due to the decomposition of small molecule hydrophilic chromogenic compounds which were originally contained in the liquid under the action of high-temperature thermal effects. At the same temperature, compared the color of the liquid obtained from mono HTL of OS with that from co-HTL of OS and BC, it was found that the addition of BC made the liquid clearer and lighter in color. This was because the porous structure of BC could adsorb organic pigment impurities in the liquid [28], and the attached microbial community on BC could immobilize and degrade macromolecular organic compounds in the liquid [29, 30].

3.2. Filtration and dehydration characteristics

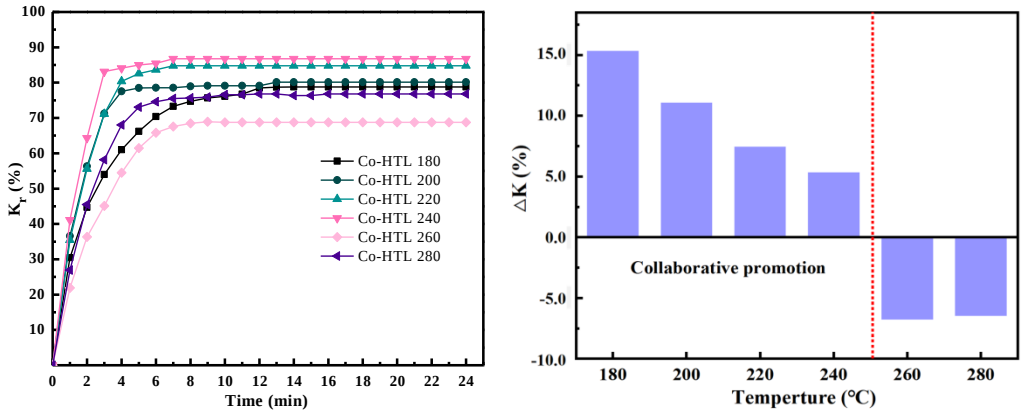

(a) Filtration characteristic curves (b) The differences of the liquid yields

Figure 3. Filtration performance in the different conditions

The filtration characteristic curves of the liquid products obtained from co-HTL of OS and BC are shown in Figure 3. (a), and the differences of the liquid yields between co-HTL and HTL are shown in Figure 3 (b). From Figure 3 (a), the addition of BC significantly increased the liquid yield and improved the filtration performance of OS at the different hydrothermal temperatures. The liquid yield increased with the extension of filtration time. Based on the previous study, the liquid percentage from raw OS without HTL after filtration was 33.81% [23]. Compared to raw OS, the liquid yield from co-HTL number was obviously more than 33.81%. As the hydrothermal temperature increases from 180 to 240 ℃, the final liquid yield obtained in the co-HTL process gradually increased, reaching the maximum value of 86.7% at 240 ^{o}C. This was because OS had a stable water-oil structure, which was destroyed under high hydrothermal temperature and pressure conditions. OS released more water, while the hydrolysis, decarboxylation, heteroatom chain breakage and other decomposition reactions that occurred during the hydrothermal process made the surface of the oil residue carbon highly hydrophobic [31]. As the HTL temperature increased further, the crushing effect of colloids and asphaltenes became more obvious. However, as the temperature continued to increase to 260 or 280 ^{o}C, the final liquid yield of OS decreased, indicating that the filtering performance of OS would be inhibited at the excessively high temperatures. The reason for this phenomenon may be due to the reactions between BC and OS at high temperature, resulting in an increase in the volume of newly generated oil residue

carbon particles, which blocked the filter holes of the filter paper and led to a decrease in the final liquid yield, and at the hydrothermal temperature of 280 ℃, this inhibition effect was most obvious. In addition, when the temperature rose to 250-300 ℃, it would cause free radicals in the hydrothermal reaction system to undergo condensation and polymerization reactions again, leading to an increase in the content of lipids and asphaltenes and inhibiting the dehydration of OS [31].

From Figure 3 (b), as the hydrothermal temperature raised from 180 to 240 ^{o}C, the differences of the liquid yields from co-HTL of OS and BC decreased from 15.35 to 5.34%, but they were more than zero. It indicated that the addition of BC into OS had a synergistic promoting effect on the hydrothermal dehydration of OS. As the hydrothermal temperature increased further, this promoting performance of BC gradually decreased, but the dehydration effect of co-HTL was still better than that of OS HTL. This was because when the temperature gradually rose, the vast majority of the colloids and asphaltenes in OS had already cracked, and the performance of releasing water gradually fully decreased [32, 33]. Therefore, the promotion effect was weakened compared to 180 ℃. When the temperature increased to 260 or 280 ℃, the differences of the liquid yields from co-HTL of OS and BC were less than zero. It was found that the addition of BC had an inhibitory effect on the hydrothermal dehydration of OS. This was due to the excessively high temperature, which deactivated effective functional groups on the surface of BC [34]. In addition, when the hydrothermal temperature increased to 260 and 280 ℃, the liquid degraded at a higher temperature and produced more hydrochars and gases. Besides, the more and bigger carbon particles generated during the hydrothermal process adhered to the hydrochar surface and reduced the specific surface area of hydrochars, making hydrochars unable to act as a conduit for the released water flow and resulting in a decrease in liquid yield [35].

3.3. Distribution characteristics of three-phase products

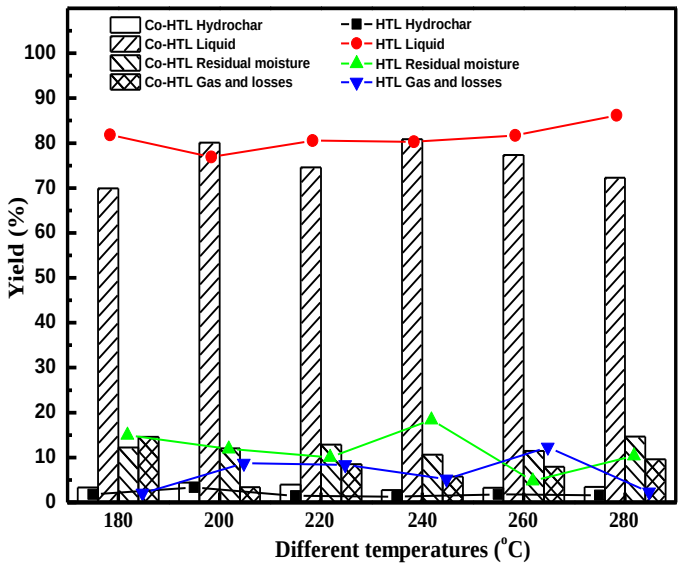

Figure 4. Comparison of product distributions under mono HTL and co-HTL

The comparison of product distributions under mono HTL and co-HTL is shown in Figure 4. From Figure 4, the hydrochar content from co-HTL was obviously more than that

from HTL at the temperature ranging from 180 to 280 °C. It indicated that the addition of BC into OS boosted the yield of hydrochars. This was because the addition of BC played a catalytic role in the entire hydrothermal system, promoting the conversion of some long-chain hydrocarbons into more stable aromatic compounds (precursors of composite hydrothermal carbon) [36]. As the hydrothermal temperature increased, the hydrochar content from the co-HTL of OS and BC increased firstly and then decreased, and it obtained the maximum value of 4.39% at 200 ℃. When the hydrothermal temperatures was at 200 or 240 °C, the liquid mass ratio from co-HTL was more than that from HTL at the same temperature, while at 180, 220, 260 and 280 °C, the result was opposite. When the hydrothermal temperature increased to 260 ℃, the mass ratio of the liquid obtained from the co-HTL treatment decreased by 4.37% compared to that of HTL, while the hydrothermal temperature was 280 ℃, it decreased by 13.92%. So, the hydrothermal temperature of 240 ℃ was the optimal reaction temperature for the co-HTL of BC and OS in this work, with a maximum liquid phase yield of 80.89%.

3.4. Characterization of the microstructure of liquid

(1) Images of mono HTL liquid at 400 × magnification

In order to improve the quality of the liquid products and promote their application in the future, studying the effects of BC addition and hydrothermal temperature on the morphology and oil compositions of the liquid phase is of great significance. The purpose of this work was to determine the optimal hydrothermal temperature for co-HTL and obtain high-quality liquid. The microscopic morphology images of the liquid products obtained from OS mono HTL are shown in Figure 5.

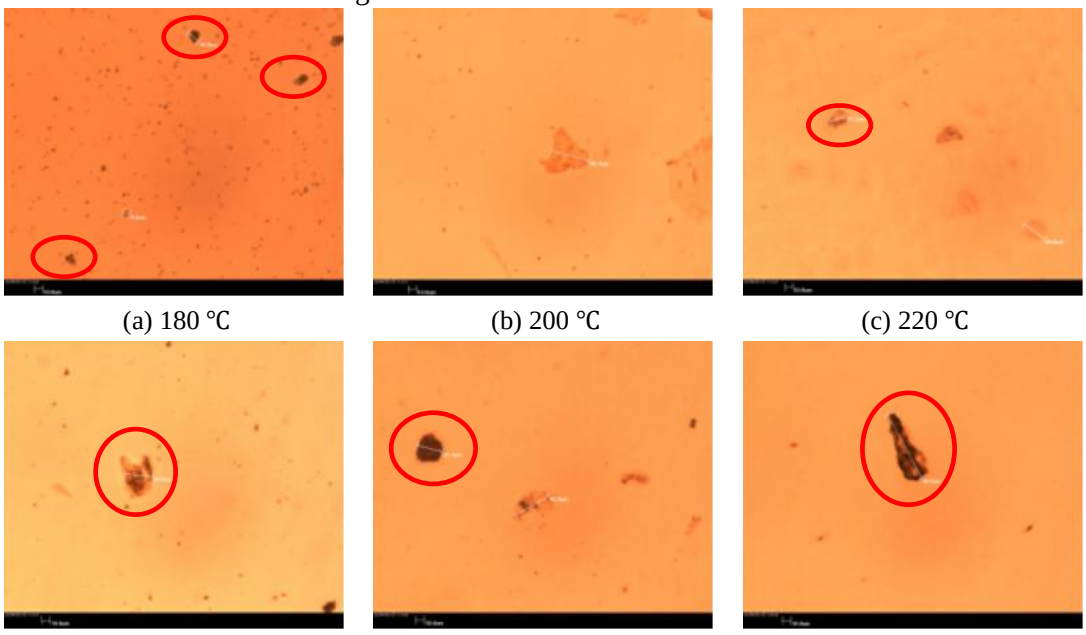

(a) 180 ℃ (b) 200 ℃ (c) 220 ℃

(d) 240 ℃ (e) 260 ℃ (f) 280 ℃

Figure 5. Microscopic images of the liquid products from OS mono HTL (400 × magnification)

It was found from Figure 5 that the hydrothermal temperature significantly affected the aqueous particles of OS. The raw OS without treatment presented clearly the internal oil-in-water emulsion structure and a large number of bubbles, thus forming a stable

emulsified flocculent liquid [37, 38]. From the Figure 5 (a)-(f), as the hydrothermal temperature increased, the original oil-in-water structure gradually disappeared after HTL treatment, which was due to the impact of thermal effects that caused the emulsion structure to break down. However, there were still large particles (red circle area) in the liquid. As the hydrothermal temperature gradually increased, the number of bubbles in the liquid obviously decreased, which was due to the degassing and precipitation of bubbles in the high temperature-pressure hydrothermal environment. In addition, the black granular substances which were named hydrochars appeared in the liquid during hydrothermal treatment at 240 to 280 ℃, which was due to the formation of oil residue carbon at high temperatures. It meant that the excessive hydrothermal temperature could made OS carbonization and produced more hydrochars.

(2) Images of co-HTL liquid at 400 × magnification

The microscopic morphology images of the liquid products obtained from OS co-HTL in the different conditions are in Figure 6. As the hydrothermal temperature increased, the color of the liquid from co-HTL of OS and BC gradually became lighter and clearer, and the number and size of black granular hydrochar particles decreased. When the hydrothermal temperature rose to 260 and 280 ^{o}C, the black particles almost disappeared, but some smaller sized agglomerates (red circle area) still appeared. The reason for this phenomenon was that OS was easily destroyed and modified during the co-HTL process of OS and BC at the higher hydrothermal temperature. The active components loaded on the modified BC played a catalytic role, weakening the bond energy of carbon-carbon bonds, making it easier for macromolecular substances to break down into small molecules (i.e. saturated and aromatic fractions) [34, 39].

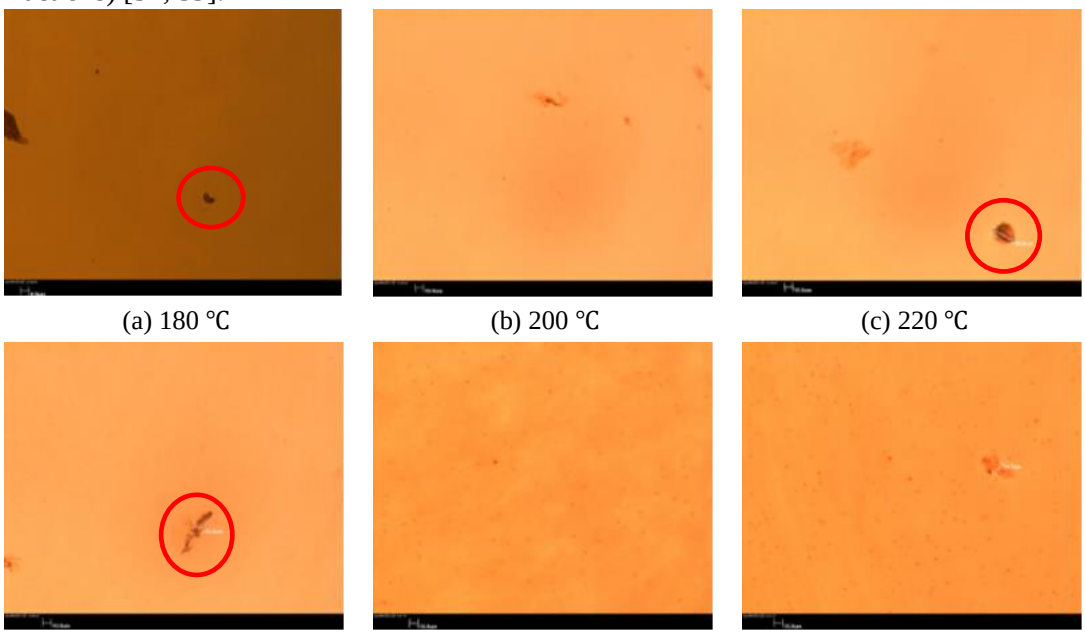

(a) 180 ℃ (b) 200 ℃ (c) 220 ℃

(d) 240 ℃ (e) 260 ℃ (f) 280 ℃

Figure 6. Microscopic images of the liquid products from OS co-HTL (400 × magnification)

From Figure 5 and 6, by comparing the micrographs of the liquid products obtained from mono HTL and co-HTL, the amount of hydrochar particles in the liquid after co-HTL

were significantly reduced. This was because the porous structure of BC adsorbed more hydrochar particles, making the liquid carry less ones [40]. From Figure 6 (e)-(f), the soluble impurities in the liquid were almost completely removed, which was due to the accelerated hydrothermal cracking and decomposition of macromolecular substances such as asphaltenes at the higher temperatures [41].

3.5. Characteristic analysis of liquid

3.5.1. Effect of adding BC on the compositions of liquid

The liquid obtained from the co-HTL of OS and BC consisted of a large amount of organic compounds, so the important compounds produced from the interactions between OS and BC were analyzed. The more detailed analysis was conducted on the liquid product from the co-HTL of OS and BC by using GC-MS. The peak area percentage of the compounds in the liquid expressed qualitatively the relative content of the ones. The changes of the compounds in the three liquid products from the mono HTL of OS and the co-HTL of OS and BC at 180 ℃ were analyzed, as shown in Figure 7. The main components of the liquid were mainly divided into anilines, alcohols, phenols, ketones, aldehydes, esters, acids, heterocyclic compounds and others.

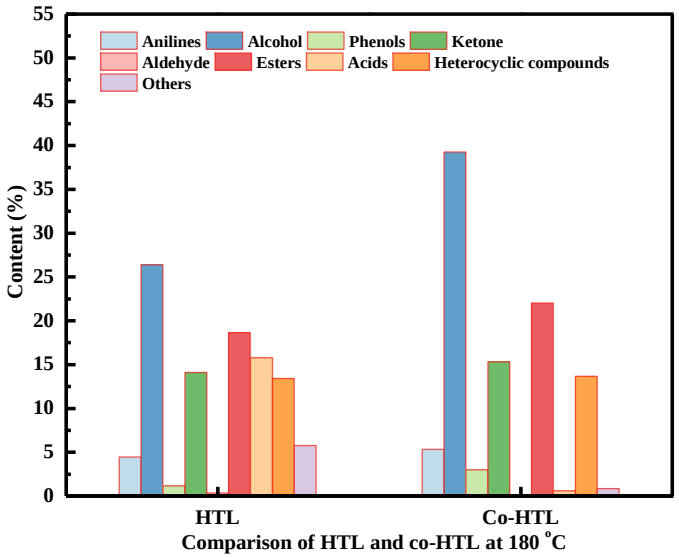

Figure 7. Compound proportion distributions of the liquid products from mono HTL and co-HTL

From Figure 7, compared with mono HTL, co-HTL treatment had the different effects on the main chemical compositions of the liquid. The relative content of alcohol increased from 26.38 of HTL to 39.27% of co-HTL, which was due to the ring opening of some oxygen-containing heterocyclic compounds in the hydrothermal reaction environment, leading to the formation of alcohol substances. The proportion values of heterocyclic compounds in the liquid obtained via HTL and co-HTL were 13.41 and 13.67%, respectively. Co-HTL had the significant impact on the content of acid and ester compounds. According to the liquid obtained from the co-HTL of OS with BC in Figure 7, the total contents of alcohols, ketones and esters from HTL and co-HTL were 59.12 and 76.61%, respectively. After HTL,

the content of others including hydrocarbon substances in the liquid significantly decreased, accounting for 5.76%, which was due to the aromatization of long-chain hydrocarbons in raw OS [13]. After co-HTL, the proportion of the others in the liquid was only 0.83%. This indicates that BC can promote the occurrence of aromatization. The content of acid compounds in the liquid increased from 5.18% of raw OS filtrate to 15.76% of HTL liquid, while the acid content in the liquid from co-HTL was only 0.7%. The large number of hydroxyl groups in BC could react with carboxyl groups, further reducing carboxyl acid content [42]. It was worth noting that after co-HTL treatment, the content of ester substances in the liquid was 22.03%, which was twice the ester content in the original liquid. This indicated that the addition of BC enhanced the esterification reaction in the hydrothermal system, with a large amount of carboxylic acids converted into esters [43]. The addition of BC had little effect on aldehydes and ketones in the liquid.

3.5.2. Effect of temperature on the compounds of co-HTL liquid

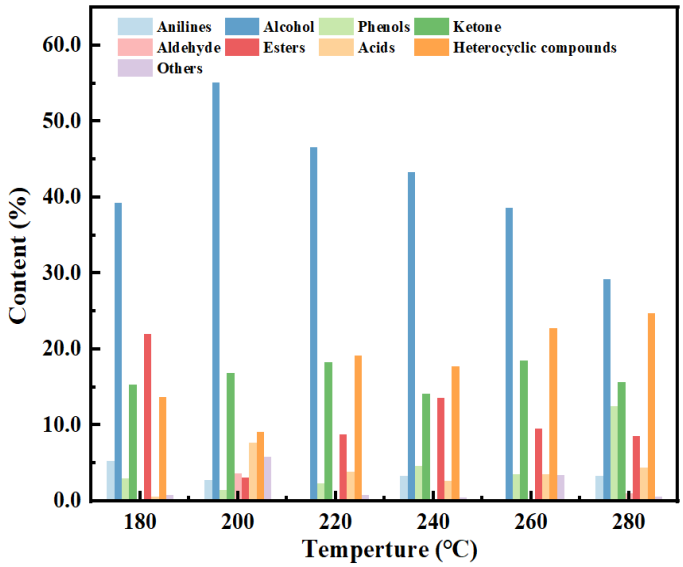

Figure 8. Compound proportion distributions of the liquid products at the different temperatures

The proportion distributions of compounds in the liquid from co-HTL at the different temperatures are presented in Figure 8. As the hydrothermal temperature increased, the content of alcohol compounds in the produced liquid firstly increased and then gradually decreased, reaching the maximum value of 55.15% at 200 ^{o}C. However, the change tendency of the content of heterocyclic compounds was opposite, with a first decreasing and then increasing trend, reaching the minimum value of 9.17% at 200 ^{o}C. This was because some oxygen-containing heterocyclic compounds gradually decomposed and opened rings with an increase of temperature, transforming into alcohols. The content of acids or ester compounds showed a fluctuating trend with the increase of temperature. Because the metal components (such as Al, Fe and other metal active sites) loaded on BC promoted the conversion of carboxylic acids to ester compounds [42]. As the hydrothermal temperature increased, the content of aniline compounds fluctuated, reaching the minimum value of 0.7%, which was due to the deamination reaction in the system and forming ammonium ion [44]. Based on the GC-MS results, the addition of BC effectively improves the product content of aromatic

alcohols in the liquid. However, the excessive hydrothermal temperature (>260 ℃) could increase the content of heterocyclic compounds.

3.5.3. Carbon number distributions in liquid

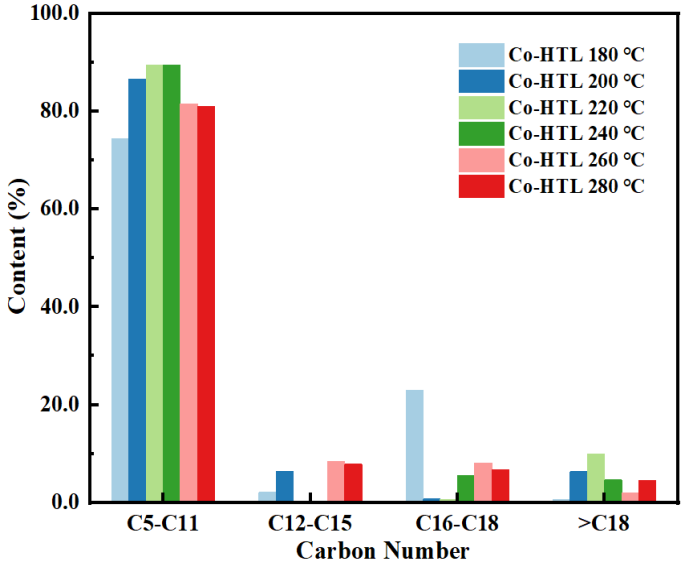

Figure 9. Carbon number distributions in the liquid products obtained from co-HTL

Generally, the carbon number of gasoline, kerosene and diesel are C5-C11, C12-C15 and C10-C22, respectively [45]. To evaluate the quality of the liquid products as fuel, the chemical compounds in the liquid products obtained from HTL were classified according to the number of carbon atom. The results of the carbon number distribution are presented in Figure 9. In Figure 9 the carbon numbers in the liquid product from co-HTL at the temperatures ranging from 180 to 280 ^{o}C were mainly distributed in C5-C11, which were the major component of gasoline. The relative content of C5-C11 at 240 ^{o}C reached the maximum value of 89.45 %. Therefore, the liquid product from co-HTL of OS and BC could be an important material in gasoline production. However, the liquid products at 220 and 240 ^{o}C didn't have the compounds containing C12-C15, and those at 200 and 220 ^{o}C had small amount of the compounds containing C16-C18. The compounds containing > C18 were obtained across the temperature range of 180 to 280 ^{o}C. So, hydrothermal temperature has a significant influence on the carbon numbers in the liquid products. Based on the above analysis, BC addition into OS would be benefit for improving the fuel performance of the liquid from OS. This is a new effective way to disposal and utilize OS in the future.

4. Conclusions

The co-hydrothermal liquefaction (co-HTL) characteristics of oily scum (OS) and poplar sawdust biochar (BC) were studied in this work. The results indicated that the addition of BC into OS improved significantly the color clarity of the liquid product. The increase of hydrothermal temperature enhanced the dewatering performance and liquid yield of OS. Alcohols were the major components of the liquid product from co-HTL of OS and BC. The carbon numbers in the liquid product from co-HTL at the temperatures ranging from 180 to

280 ^{o}C were mainly distributed in C5-C11. The liquid product from co-HTL is used as an important material in gasoline production. 240 ^{o}C is considered the optimal reaction temperature in the co-HTL of OS and BC in this work, at which the liquid yield and the concentration of the compounds containing C5-C11 reach the maximum values. The results obtained in this work can offer basic experimental data and important reference for the treatment and utilization of OS.

Acknowledgements

This research has received the support of the Basic Research Program of Natural Sciences of Shaanxi Province (No. 2023-JC-YB-406).

References

[1] Yuan, X. Z., et al., Effective treatment of oily scum via catalytic wet persulfate oxidation process activated by Fe^{2+}, *Journal of Environmental Management*, 217 (2013), Jul, pp. 411-415.

[2] Y. Liu, et al., Co-pyrolysis of sewage sludge and lignocellulosic biomass: Synergistic effects on products characteristics and kinetics, *Energy Conversion and Management*, 268 (2022), Sep, 116061.

[3] Dilnur, M., et al., Discussion on the Prospect of Reused Technology of Oily Sludge, *Guangzhou Chemical Industry*, 41 (2013),14, pp. 3-5.

[4] Guo, S.H., et al., Improvement of acidification on dewaterability of oily sludge from flotation, *Chemical Engineering Journal*, 168 (2011), 2, pp. 746-751.

[5] Zhang, L., et al., Process for the Reduction of High Water Content from Oily Sludge and Scum by Hot Washing, *Nature Environment and Pollution Technology*, 22 (2023), 3, pp. 1125-1137.

[6] Mishra, S., et al., In situ bioremediation potential of an oily sludge-degrading bacterial consortium, *Current Microbiology*, 43 (2001), 5, pp. 328-335.

[7] Shi, B. W., et al., Co- Combustion of Oil Sludge Char and Brown Coal in a Continuous Fluidized- Bed Combustor, *Chemie Ingenieur Technik*, 95 (2022),1-2, pp. 77-88.

[8] Li, J. T., et al., Transformation and regulation of nitrogen and sulfur during pyrolysis of oily sludge with N/S model compounds, *Fuel*, 324 (2022), Sep, 124651.

[9] Zhao, R. D., et al., Experimental study on co-combustion of low rank coal semicoke and oil sludge by TG-FTIR, *Waste Management*, 116 (2020), Oct, pp. 91-99.

[10] Cao, Y. H., et al., Synergistic effect, kinetics, and pollutant emission characteristics of co-combustion of polymer-containing oily sludge and cornstalk using TGA and fixed-bed reactor, *Renewable Energy*, 185 (2022), Feb, pp. 748-758.

[11] Deng, S. H., et al., The Effect of Hydrothermal Dewatering Temperature on Hydro-Char Obtained from Oily Scum, *Materials Science Forum*, 971 (2019), Sep, pp. 127-133.

[12] Neyens, E., et al., A review of thermal sludge pre-treatment processes to improve dewaterability, *Journal of Hazardous Materials*, 98 (2003), 1-3, pp. 51-67.

[13] Zhang, J., et al., Co-hydrothermal carbonization of polyvinyl chloride and lignocellulose biomasses for chlorine and inorganics removal, *Waste Management*, 156 (2023), Feb, pp. 198-207.

[14] Wang, R. K., et al., The redistribution and migration mechanism of nitrogen in the hydrothermal co‐carbonization process of sewage sludge and lignocellulosic wastes, *Science of The Total Environment*, 776 (2021), 145922.

[15] Zhong, J., et al., Hydrothermal carbonization of coking sludge: Formation mechanism and fuel characteristic of hydrochar, *Chemosphere*, 346 (2023), Jan, 140504.

[16] Duan, Y. W., et al., Subcritical hydrothermal purification from oily sludge recovered from petroleum oily sludge by adding sodium hydroxide, sodium bicarbonate, and formic acid, *Environmental Progress & Sustainable Energy*, 42 (2023), 6, e14220.

[17] Namioka, T., et al., Hydrothermal treatment of dewatered sewage sludge cake for solid fuel production, *Journal of Environment and Engineering*, 4 (2009), 1, pp. 68-77.

[18] Zhang, S., et al., Influence of sodium hypochlorite/ultrasonic pretreatment on sewage sludge and subsequent hydrothermal liquefaction: Study on reaction mechanism and properties of bio-oil, *Biomass & Bioenergy*, 175 (2023), Aug, 106872.

[19] Cavali, M., et al., Co-hydrothermal carbonization of pine residual sawdust and non-dewatered sewage sludge - effect of reaction conditions on hydrochar characteristics, *Journal of Environmental Management*, 340 (2023), Aug, 117994.

[20] Shan, G. C., et al., Co-hydrothermal carbonization of agricultural waste and sewage sludge for product quality improvement: Fuel properties of hydrochar and fertilizer quality of aqueous phase, *Journal of Environmental Management*, 326 (2023), Jan, 116781.

[21] Mahata, S., et al., A review on Co-Hydrothermal carbonization of sludge: Effect of process parameters, reaction pathway, and pollutant transport, *Journal of the Energy Institute*, 110 (2023), Oct, 101340.

[22] Zhang, Q., et al., Low nitrogen and high value hydrochar preparation through co-hydrothermal carbonization of sludge and saw dust with acid/alcohol assistance, *Energy*, 278 (2023), Sep, 128012.

[23] Deng, S. H., et al., Experimental investigation of the dewatering performance and product characteristics of oily scum at increased reaction time through hydrothermal treatment, *Asia-Pacific Journal of Chemical Engineering*, 17 (2022), 1, e2737.

[24] Hu, J. X., et al., Understanding the impact of pectin physicochemical variation on browning of simulated Maillard reaction system in thermal and storage processing, *International Journal of Biological Macromolecules*, 240 (2023), Jun,124347.

[25] Nakamura, M., et al., Browning of Maillard reaction systems containing xylose and 4-hydroxy-5-methyl-3(2H)-furanone, *Bioscience Biotechnology and Biochemistry*, 85 (2021), 2, pp. 401-410.

[26] Yang, N., et al., Exploration of browning reactions during alkaline thermal hydrolysis of sludge: Maillard reaction, caramelization and humic acid desorption, *Environmental Research*, 217 (2023), Jan, 114814.

[27] Wang, Q. D., et al., Mechanistic insights into the effects of biopolymer conversion on macroscopic physical properties of waste activated sludge during hydrothermal treatment: Importance of the Maillard reaction, *Science of the Total Environment*, 769 (2021), May, 144798.

[28] R. Wolski, et al., Adsorption of methyl red and methylene blue on carbon bioadsorbents obtained from biogas plant waste materials, *Molecules*, 28 (2023), 18, 6712.

[29] Yu, L. P., et al., Biochar as an electron shuttle for reductive dechlorination of pentachlorophenol by Geobacter sulfurreducens, *Scientific Reports*, 5 (2015), Nov, 16221.

[30] Mohan, D., et al., Organic and inorganic contaminants removal from water with biochar, a renewable, low cost and sustainable adsorbent – A critical review, *Bioresource Technology*, 160 (2014), May, pp. 191-202.

[31] Al-Muntaser, A. A., et al., Hydrothermal upgrading of heavy oil in the presence of water at sub-critical, near-critical and supercritical conditions, *Journal of Petroleum Science and Engineering*, 184 (2020), Jan, 106592.

[32] Yang, J. P., et al., Deep dewatering of refinery oily sludge by Fenton oxidation and its potential influence on the upgrading of oil phase, *Environmental Science and Pollution Research*, 30 (2023), 31, pp. 76617-76630.

[33] Rukomoynikov, A. A., et al., Agliullin, Energy-Efficient Separation of Water–Petroleum Emulsion, *Russian Engineering Research*, 42 (2022), Oct, pp. 916-919.

[34] Wang, Y. Y., et al., ZrO2-MoO3/modified lotus stem biochar catalysts for catalytic aquathermolysis of heavy oil at low-temperature, *Fuel*, 357 (2024), Feb, 129597.

[35] Wang, J. X., et al., Deep dewatering of sewage sludge and simultaneous preparation of derived fuel via carbonaceous skeleton-aided thermal hydrolysis, *Chemical Engineering Journal*, 402 (2020), Dec, 126255.

[36] Zhang, J. B., et al., Catalytic hydrothermal liquefaction of alkali lignin for monophenols production over homologous biochar-supported copper catalysts in water, *International Journal of Biological Macromolecules*, 253 (2023), Dec, 126656.

[37] Liu, W., et al., Emulsions stabilized by asphaltene-polyacrylamide-soil three-phase components: Stabilization mechanism and concentration effects, *Separation and Purification Technology*, 302 (2022), Dec, 122157.

[38] Chen, Z., et al., Oily sludge treatment in subcritical and supercritical water: A review, *Journal of Hazardous Materials*, 433 (2022), Jul, pp. 128761.

[39] Zhao, Y. L., et al., Hydrothermal pretreatment of cotton textile wastes: Biofuel characteristics and biochar electrocatalytic performance, *Fuel*, 316 (2022), May, 123327.

[40] Zakieva, R. R., et al., Hydrothermal Transformation of Superviscous Oil in the Presence of Coals, Metal Oxides, and Carbonates, *Chemistry and Technology of Fuels and Oils*, 59 (2023), 1, pp. 69-74.

[41] Kayukova, G. P., et al., Changes of Asphaltenes' Structural Phase Characteristics in the Process of Conversion of Heavy Oil in the Hydrothermal Catalytic System, *Energy & Fuels*, 30 (2016), 2, pp. 773-783.

[42] Cao, B., et al., Seaweed-derived biochar with multiple active sites as a heterogeneous catalyst for converting macroalgae into acid-free biooil containing abundant ester and sugar substances, *Fuel*, 285 (2021), Feb, 119164.

[43] Zhang, X., et al., Production of acid-free bio-oil through improved co-HTL of sludge and microalgae: Experiment and life cycle assessment, *Journal of Cleaner Production*, 379 (2022), Dec, 134668.

[44] Robinson, K. J., et al., Deamination reaction mechanisms of protonated amines under hydrothermal conditions, *Geochimica et Cosmochimica Acta*, 244 (2019), Jan, pp. 113-128.

[45] Mousavi, S., et al., Catalytic pyrolysis of plastic waste to gasoline, jet fuel and diesel with nano MOF derived-loaded Y zeolite: Evaluation of temperature, zeolite crystallization and catalyst loading effects, *Energy Conversion and Management*, 299 (2024), Jan, 117825.

Paper submitted: 27.05.2024
Paper revised: 30.06.2024
Paper accepted: 05.07.2024